Proceedings of OMAE2009
28th International Conference on Offshore Mechanics and Arctic Engineering
May 31- June 5, 2009, Honolulu, Hawaii

OMAE2009-79801

NUMERICAL MODELING OF VORTEX-INDUCED VIBRATIONS OF TWO FLEXIBLE RISERS

Marlow Springer
ACUSIM Software, Inc.
Mountain View, CA 94043

Rajeev K. Jaiman
ACUSIM Software, Inc.
Mountain View, CA 94043

Steve Cosgrove
ACUSIM Software, Inc.
Mountain View, CA 94043

Yiannis Constantinides
Chevron Energy Technology Company

ABSTRACT

Due to the complex interactions of vortex-induced vibrations (VIV) and downstream wake dynamics, the design of riser arrays has been an area of great uncertainty in the offshore industry. Numerical methodology can play an important role in predicting the hydrodynamic forces and motion of riser arrays from both design and operational standpoints. The focus of this study is to investigate the VIV response of two flexible risers in cross-flow using a CFD solver. Bare and straked geometries are simulated, and the results are successfully compared against experimental results. The basic hydrodynamic features are well captured and the numerical technique is an improvement over the existing empirical and experience-based methods.

INTRODUCTION

Fluids flows passing over flexible cylinders arise in numerous offshore engineering situations, such as marine risers, mooring lines, spars, cables etc. Significant progress has been made in understanding the wake and the vortex induced vibration (VIV) of a long single cylinder using fully three dimensional fluid flow simulations with a simple structural model [1,2]. The interactions and collisions of the risers are a source of concern in offshore developments. Until now, the usual practice has been to design the risers with sufficient spacing to avoid contact as they move in the ocean current. But avoiding interaction in this manner may not be practical or economical as production moves to deeper water.

Recently, experimental and simulation studies have done about the behavior of arrays of flexible cylinders subjected to VIV [3,4,5]. These articles highlight the various phenomena associated with VIV and lock-in of two cylinders in tandem arrangement. Lock-in is observed for a range of structural frequencies of the risers; the vortex shedding frequency of an oscillation cylinder changes to the structural frequency as a result of the VIV. Apart from the flow conditions and structural properties, the relative locations of the cylinders play an important role in the vortex shedding and synchronization (lock-in).

The behavior of riser arrays in ocean currents is a complex hydroelastic problem and can be characterized in terms of structural motion with different time scales. Low coupled modes generally determine long periodic translations, while high-frequency VIV motions occur at much higher modes. The low coupled mode shapes are generally related to wake induced oscillations. Flow separations and partial shielding by upstream risers can significantly alter the local fluid behavior in terms of amplitude, frequency and phase as compared to a single riser analysis. Moreover, the flow approaching the downstream riser is generally turbulent. As a result, the differences and interactions of excitation of adjacent cylinders may produce large relative motions that can bring them into contact. In addition, high levels of VIV fatigue damage can be accumulated in relatively short periods of time in operational environments. Methods and models for predicting the

probability of riser collisions and the resulting hydrodynamic forces are generally needed.

Due to the complexity of the hydroelastic cylinder/wake problem, theoretical and semi-empirical models remain incomplete. Recently, numerical simulation has emerged as an efficient tool with high accuracy for studying VIV at high Reynolds numbers. Therefore, the process of developing a numerical methodology and comparing the numerical results with full-scale measurements has a great significance to the offshore industry.

In [1,2], a detailed analysis has been presented for the vortex induced vibration (VIV) of a long single riser using fully three-dimensional fluid flow simulations with a simple structural mode. This paper reports a continuation of that work to simulate two tandem flexible risers in cross-flow and compares the results with experimental data. We attempt to use fully three-dimensional CFD simulations coupled with relatively simple and linear structural models to predict the VIV of two risers. The objective of this study is to clarify the accuracy of the numerical simulation. Two configurations are studied: two bare risers and two straked risers.

In the following sections we describe the general method of solution combining 3D fluid flow solutions with a structural model. The problem of creating an optimal mesh is discussed in which the objective is to combine acceptable solution accuracy with good solution economy. We then describe benchmark calculations - comparing the predicted response of the two bare and straked risers with laboratory experiments.

NOMENCLATURE

A = motion amplitude [m]
D = riser diameter [m]
L = riser lenght [m]
x, y, z = coordinates [m]
U = current velocity; maximum for sheared profile [m/s]
$Re = UD/\nu$ = Reynolds number [-]
$V_{rm} = U/fnD$ = Nominal reduced velocity [-]
t = time [s]
K_i^n = riser stiffness matrix
m_i^n = riser mass matrix
n = mode number
S_i^n = eigenvector
T_i = Surface traction
ξ_i = Eigenvector of ith mode

NUMERICAL METHODOGLOGY

All of the solutions shown here were produced using the AcuSolve™ finite element Navier-Stokes solver [7]. AcuSolve™ is based on the Galerkin/Least-Squares formulation and supports a variety of element types. AcuSolve™ uses a fully-coupled pressure/velocity iterative solver plus a generalized alpha method as a semi-discrete time stepping algorithm. AcuSolve™ is second order accurate in space and time. Turbulence is modeled using the detached eddy simulation model [8]. In his model, we resolve the large eddies that have the biggest effect on the forces on the riser and use wall functions to describe the flow at the wall in all CFD simulations. This was done not only to economize on mesh size, but also because most risers have relatively rough walls. Wall functions reduce mesh size by providing an integrated relationship between the wall and the logarithmic region of the boundary layer. A more detailed discussion of the turbulence model and the wall treatment is given in [1].

The problem of riser motion is solved using a simple linear vibration analysis and the displacements from the riser mean position are assumed small. The displacement is characterized by normal modes of vibration found using an eigenvalue analysis. The displacements of the riser are then a linear sum of the modal amplitudes times the corresponding eigenvectors. In the problems solved here, the riser axis is oriented in the z-direction and we assume the eigenmodes to be sinusoidal so the eigenvectors have the form:

$$S_i^n(z) = \sin\left(\frac{n\pi z}{L}\right) \quad \textbf{(1)}$$

where the S_i^n is the eigenvector associated with the nth mode and the i index indicates the x or y directions in this case, L is the riser length, z is the distance along the riser axis and n is the mode number. It should be noted that the risers modeled here are tension dominated - the bending stiffness of the riser is negligible compared to the stiffness due to tension. Also, the use of a sine shape in [1] implies that the riser tension is constant along the riser length.

With this approach, the motion of the riser is assumed to be a linear summation of the vibration modes. The response is found by solving the equation:

$$\left[m_i^n\right]\{\ddot{\xi}_i^n\} + \left[K_i^n\right]\{\xi_i^n\} = f_i^n \quad \textbf{(2)}$$

where ξ_i^n are the modal amplitudes, with m_i^n and K_i^n being the associated mass and stiffness of each mode. Here we chose not to model the material damping of the riser structure because it is unknown. The presumed amount of damping is less than 1% and did not affect the solution in testing here.

At each time step, the surface tractions on the riser are projected onto the eigenvectors to find the values f_i^n:

$$f_i^n = \int_A T_i(x,y,z)\cdot S_i^n(z)\,dA \quad \textbf{(3)}$$

The resulting f_i^n are then used with Equation [2] to find the model amplitudes (ξ_i^n) and the displacements for the next time step using numerical integration based on the trapezoidal rule. The mesh motion required to accommodate the changes in riser geometry were accomplished by explicitly controlling the motion of each node in the mesh. Finally, the time step for the calculations is constant and is chosen to resolve the fluid flow as accurately as possible. For the meshes used here the time step used is varied from 0.01s to 0.005s so about 100 time steps are used in a vortex shedding cycle in a typical calculation.

NUMERICAL MODELING

Model Description

The geometry is created to enable simple modification of riser locations, diameters, and strake characteristics. Figure 1 shows the overview of bare and straked riser configurations. For the simulation models, the cylinder diameter is D=0.0762 meter and the length is 26D. The risers are offset 10D in the streamwise direction with no lateral offset. The inlet boundary is positioned 10D upstream of the first riser. The outlet is 30D downstream of the second riser. The top and bottom boundaries are 15D from the risers. In the case of the straked risers, there are 3 fins with a pitch of 17D and strake height of 0.28D. In both cases, the flow current velocity is V_c =1.5 m/s. This flow speed corresponds to a Reynolds number Re=10^5 (sub-critical range) based on the diameter. Prescribed velocity boundary conditions are used on the inflow, while at the downstream end of the domain, outflow pressure conditions are used.

The shedding frequency for the single cylinder, in the absence of structural motion, can be estimated from the Strouhal equation. With Strouhal number St =0.17 at Reynolds number Re=10^5, the vortex shedding for the bare cylinder is given by: $f_v = StV_c / D = 3.34Hz$ (assuming 2-DOF motion). The analytical modal frequency of nth mode for a pinned-pinned beam can be estimated by

$$f_s^n = \frac{(n\pi)^2}{2\pi L^2}\sqrt{\left(\frac{EI}{m}\right)} \qquad n = 1,2,3,\cdots \qquad \textbf{(4)}$$

where EI and m denote the modulus of elasticity multiplied by the area moment of inertia and the mass per unit length, respectively. Table 1 summarizes the nominal reduced velocity (V_{rm}) at the current velocity, the lock-in nominal reduced velocity and the frequency ratios assuming St=0.17 for the bare and St=0.11 for the straked upstream riser. The upstream bare riser operating in near lock-in conditions but the straked is away from lock-in. We also note that it is difficult to define the shedding frequency for a straked cylinder and lock-in as it doesn't experience significant VIV.

Table 1: Physical properties and frequencies of the risers

Geometry	Vrn	1/St	f_s/f_v
Bare	6.8	5.9	0.8
Strake	6.5	9.1	1.4

Mesh Design

The approach taken here assumes that the fluid flow over the riser must be described using a three dimensional flow solution. No attempt is made to compromise the solution using quasi-three dimensional methods or other simplifications. Obtaining an economical solution is then simply finding the minimum number of degrees of freedom in the flow solution that captures the salient fluid flow effects and predicts the loads on the riser with sufficient accuracy. This problem has three parts: the resolution of the boundary layer, the resolution of the near wake and the resolution of the far field. A variety of mesh resolutions have been used here in an attempt to find the most economical mesh, but all have the same general appearance as the mesh shown in Fig. 1.

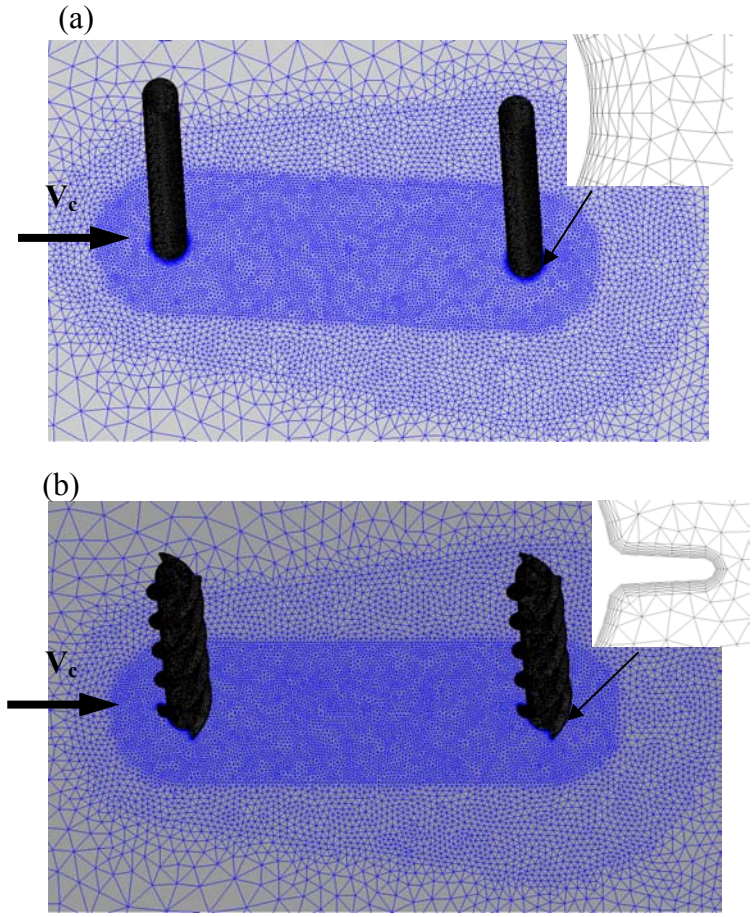

Figure 1. Geometry and mesh (a) bare risers (b) straked risers with a close-up view of boundary layer resolution.

Note that this cross section of the mesh has a wide wake region with distinct zones that are finer near the riser and coarser in the far wake. Large elements are used near the boundaries. The actual relative problem size depends on the configuration and the relative number of straked and bare lengths of riser. In general, from 4,000 to 4,500 nodes are required for every diameter of riser length.The volume closest to and between the risers has an absolute mesh size of 0.1 D. The largest elements in the mesh are 1.6D with gradual size growth in-between controlled by the other volume sizes. The surfaces of the cylindrical riser have an element size of 0.066D. The bare case has seven boundary layers off the risers (Fig. 1a). The near-wall height is 0.0066D, and the growth ratio is 1.4. This yields a mesh with roughly 1 million nodes and 6 million tetrahedral elements.

The straked case has slightly different parameters for the boundary layers. The boundary layer consists of only 5 layers instead of 7 in the bare case and the first element height is 0.0046D (see Fig. 1b). The growth ratios vary from 1.15 to 1.25 for the cylinder and strake portions. Again, these parameters along with the specific shape of the strakes seem to provide a consistent set of boundary layers with reasonable quality. This yields a mesh with roughly 1.2 million nodes and 6.9 million tetrahedral elements. Figure 1 also shows the mesh close to the risers for the bare and straked cases

SIMULATION OF TWO BARE RISERS

The first simulation is performed for the array of two bare risers in uniform flow. Although we have not performed extensive case studies, this simulation can provide a good picture of the successes and failures of the numerical approach. The vortex shedding frequency of the stationary cylinders (f_v) is close to the structural eigen-frequency (f_s) with a ratio f_s/f_v.=0.8. A soft lock-in phenomenon can occur in this case where vortex shedding frequency of the cylinders is synchronized with the structural frequency.

Figure 2 shows a visualization of the deformed risers and flow field with velocity magnitude contours in the cross-section area at t = 1.26 sec. It nicely highlights the turbulent wake dynamics and a significant influence of riser motions on the flow field. The vortex shedding from the two risers is almost anti-phase, i.e., as the first riser sheds a vortex from the upper surface, the second sheds a counter-rotating vortex from the lower surface. The response of the upstream riser is somewhat similar to that of the single riser. The downstream riser lies in the unsteady wake of the upstream riser and experiences a galloping/flutter type of physical instability. The amplitudes of the oscillations are larger for the upstream riser. Next we quantify the VIV motion of bare risers in in-line (IL) and cross-flow (CF) directions for the upstream (left) and downstream (right) risers.

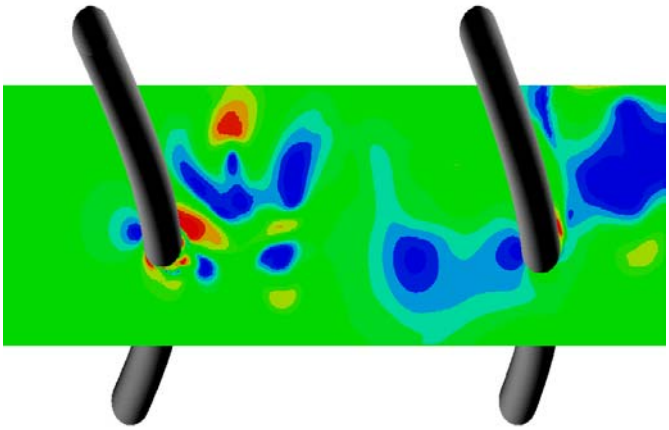

Figure 2. Instantaneous snapshot of velocity magnitude contours for two deformed bare riser

Response Prediction

The stream-wise/in-line and cross-stream displacements at the mid-span location of the risers are tracked as a function of simulation time. Figure 3(a) shows the calculated stream-wise deviation from the average position as a function of time for the bare upstream and downstream risers. The simulation was run for a dimensionless time: $tV_c/D \approx 108$. As expected, due to the wake and shielding effects of the upstream riser, the in-line deflection of the downstream riser is less than the upstream riser. Similarly the oscillation amplitude (DN-IL) of the downstream riser is less than the upstream riser (UP-IL).

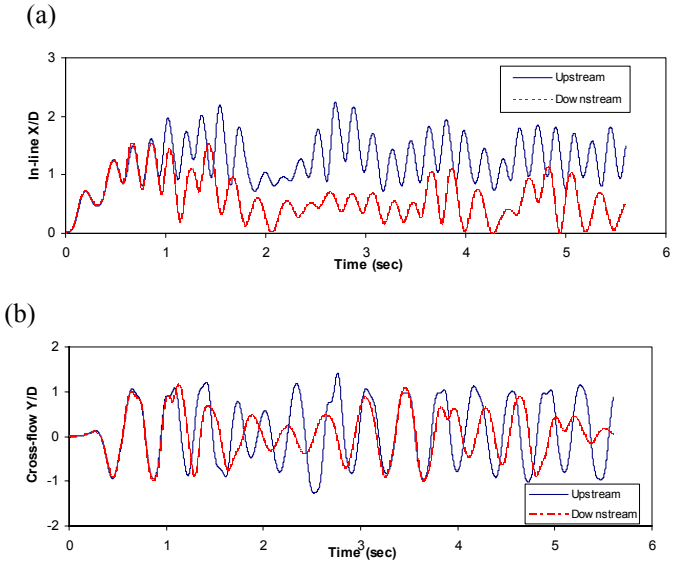

Figure 3. Time history of VIV motion at riser midpoint from (a) streamwise/in-line displacement (b) cross-flow displacement.

Figure 3(b) shows the calculated cross-stream displacements for the upstream (UP-CF) and downstream (DN-CF) risers. Similar to the in-line response, the deviations from average are smaller for the downstream riser. This is partly because the wake zone pressure is less than the pressure distribution at the upstream region. It is also noteworthy that the downstream riser motion is quite periodic which is related to the periodic unsteady behavior of wake oscillations from the upstream riser in this Reynolds number range.

Figure 4 shows the comparison of normalized nominal $\left(A^* = \sqrt{2}A_{std}\right)$ computed amplitude A^*/D response for the numerical prediction and experiment. In the plot, the straight solid line represents the perfect match of data. The amplitude responses from the prediction agree reasonably well with the experiment.

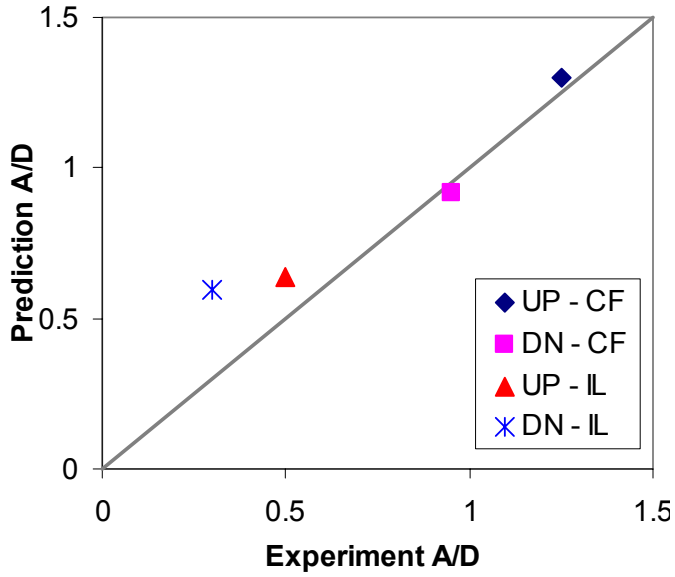

Figure 4. Nominal oscillation amplitude responses for numerical prediction and experiment where straight line represents the ideal match between the data

Force Prediction

Figure 5 shows the time variation of computed inline (drag) and crossflow (lift) forces for the two bare risers. There are several interesting features of the risers system that can be seen in these traces.

In this Reynolds number range, the boundary layer may remain laminar, although the wake may be completely turbulent. Drag in this range is primarily due to the asymmetry of the pressure distribution caused by separation.

The upstream riser has a higher average drag force and more variation than the downstream riser as shown in Fig. 5(a). The reduction of the downstream drag force is primarily due to the reduction in incident stream velocity caused by the wake deficit from the upstream riser. Figure 5(b) shows the computed crossflow forces for the bare risers. As with the drag, the downstream riser generally has a lower force, but the difference is not substantial.

(a)

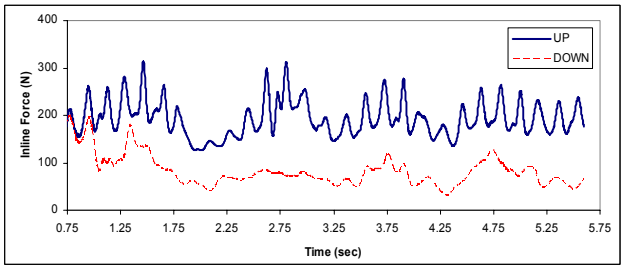

(b)

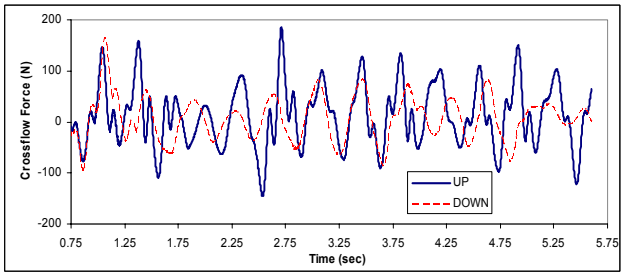

Figure 5. Time variation of integrated forces for upstream and downstream bare risers (a) inline and (b) crossflow force.

SIMULATION OF TWO STRAKED RISERS

The second simulation is performed for the array of two straked risers in uniform flow. The presence of the strakes tends to disrupt the vortex shedding and reduce the motions on the straked end of the riser while the bare end produces somewhat higher amplitudes. The vortex shedding frequency of the stationary riser (f_v) is away from the structural eigen-frequency (f_s) with a ratio f_s/f_v.=1.4.

Figure 6 shows a cross-section of the deformed risers and velocity magnitude contours at t = 5.16 sec. The plot nicely highlights the wide range of velocity scales and a significant influence of riser motions on the flow field. More importantly, the impact of strakes on the suppression of VIV can be seen on the motion of the upstream riser. Next we quantify the VIV motion of straked risers in in-line (IL) and cross-flow (CF) directions for the upstream (left) and downstream (right).

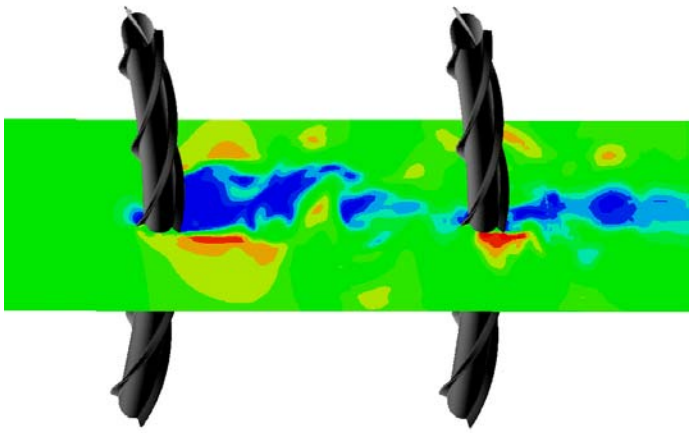

Figure 6. Instantaneous snapshot of velocity magnitude contours for two strake risers (top view) and deformed configuration of risers

Dynamic Response

Figure 7 (top) shows the calculated stream-wise/in-line offset from the initial position as a function of time for the straked upstream riser. The average position is computed from t = 2 sec to t = 5 sec, to match the 3 sec of data available from the experiment. The response before t = 2 seconds is ignored as during this time the flow is developing and has some initial conditions effects.

Figure 7 (bottom) shows the cross-stream deviations for the upstream straked riser. The upstream straked riser experiences very little VIV compared to the upstream bare riser. This implies that the strakes successfully mitigate the VIV. In fact, the upstream straked riser behaves like a single riser. However, the wake induced oscillations (large modes) have impact on the motion of the downstream riser. Moreover, the periodic wake dynamics make the strakes less effective by losing some of their ability to suppress VIV.

Figure 8 (top) shows the computed deviation from the mean stream-wise displacements for the downstream straked riser, while Figure 8 (bottom) shows the experimental deviations. Note again that the experimental run time is shorter than the simulation time. The computed deviations from the average in the simulation time between 2 and 5 seconds compare reasonably well to the experimental results.

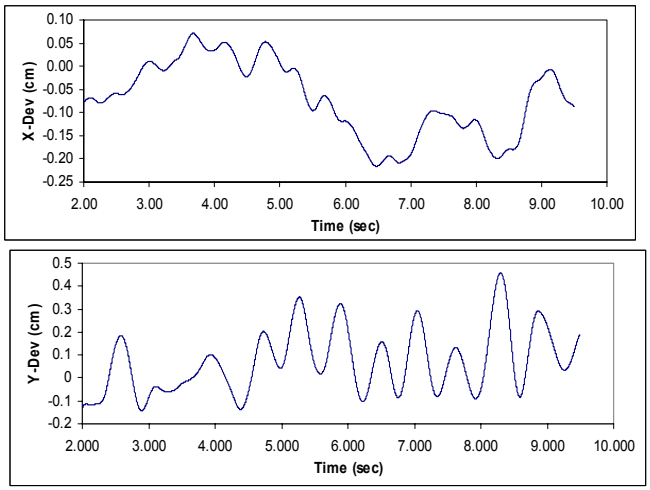

Figure 7. Upstream strake riser results for stream-wise deviation (top) and cross-stream (bottom).

Figure 9(a) shows the computed deviation from the mean cross-stream displacements for the downstream straked riser, while Figure 9(b) shows the experimental deviations. The amplitude evolution in the simulation is of the same magnitude (though somewhat larger) as observed in the experiments. The simulations are currently continued and will be repeated on a finer grid for a one-to-one comparison of the amplitude evolution with the experimental data. As noted above, the experimental run-time is shorter than the simulation time.

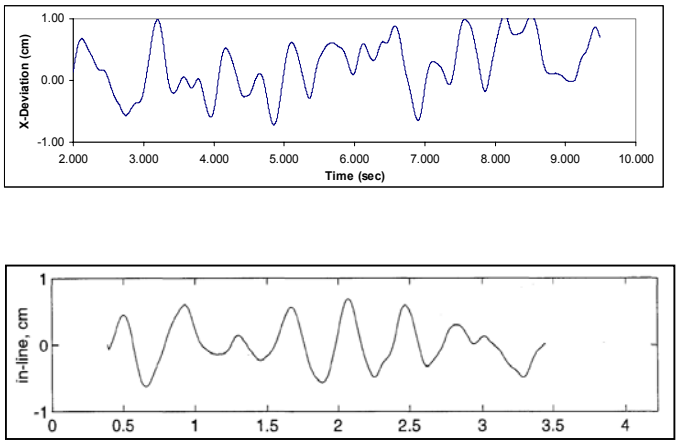

Figure 8. Computed (top) and experimental (bottom) deviation from the mean stream-wise downstream straked riser displacement

Looking at roughly the three seconds of simulation time starting where the motion 'stabilizes' at 2.0 seconds, the deviations compare reasonably well with the experiments. However, as the simulation proceeds, the motion increases to 2-3 times the experimental values. It is possible that a longer

experimental run time would also show the increased motion, but that is only conjecture at this point.

(a)

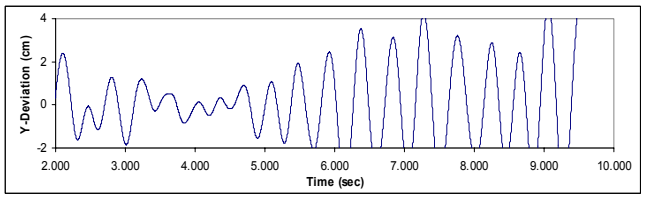

(b)

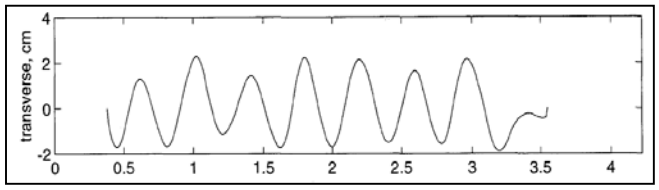

Figure 9. Mean cross-stream displacement for downstream straked riser (a) computed (b) experimental

Figure 10 shows the comparison of normalized computed amplitude A/D response for the numerical prediction and experiment for the straked risers. In the plot, the straight solid line represents the perfect match of data. For the downstream crossflow case both the 2 to 5 seconds (hollow point) and 2 to 9 seconds (solid) datapoints are included from the simulation signal. The 2 to 9 seconds record, despite being longer than the experimental, captures the couple response. The amplitude responses from the prediction agree reasonably well with the experiment.

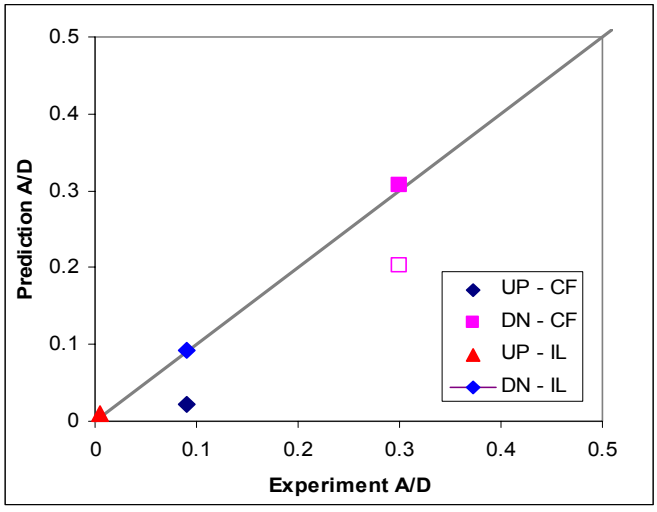

Figure 10. Nominal oscillation amplitude responses for numerical prediction and experiment where straight line represents the ideal match between the data.

Force Prediction

Figure 11(a) shows the computed drag coefficient for the straked risers. Like the bare case, the upstream riser has a higher drag coefficient; however, the downstream riser shows much less reduction in force compared to the bare case. This is due to the increase of the downstream VIV response that leads to an increase in drag force.

Figure 11(b) shows the computed crossflow force for the straked risers. The downstream riser shows much more variation in crossflow forces than does the upstream riser as it experiences more VIV. A nonzero mean crossflow force is also noted due to the nonsymmetrical straked geometry.

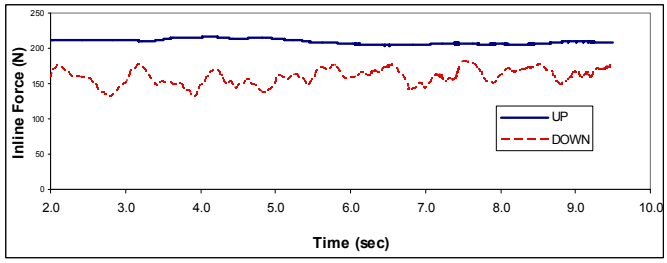

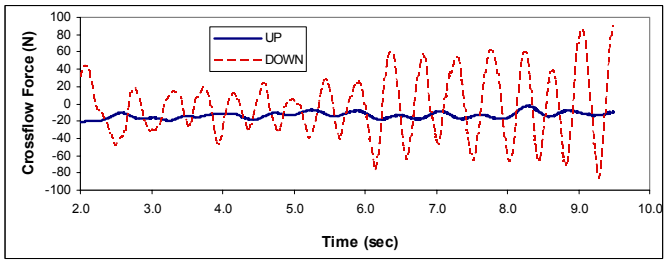

Figure 11. Computed inline and crossflow forces for upstream and downstream strake risers.

CONCLUSIONS

A fully three-dimensional CFD model was developed and coupled with a simple structural model to predict the complex VIV of a flexible riser array in cross-flow. The possibility of numerical predictions for such complex hydroelastic problems with turbulent wakes is shown in this study.

The numerical simulations have done a reasonable job predicting the qualitative responses of the experiments, and even exhibiting acceptable quantitative agreement for the bare riser upstream and downstream responses, and the straked downstream stream-wise (in-line) response. The case with bare risers showed that both risers exhibited similar motions while the upstream riser had slightly higher amplitude and variation in the motion. The wake dynamics of the upstream riser has impact on the motion of the downstream riser. The case with the straked risers showed that the upstream riser had very little motion whereas the downstream riser had motions

several times higher than the upstream. This suggested that when a straked riser resides in the wake of another riser, the strakes lose some of their ability to suppress VIV.

Flow interference between upstream and downstream risers and wake induced oscillations cause a change in the characteristic of fluid forces. For both bare and straked risers, the downstream drag force is lower than the upstream. The downstream crossflow force is slightly reduced in amplitude compared to the upstream. On the other hand, the downstream straked cylinder force is significantly amplified compared to the upstream. A quantitative benchmark study is in order to compare the predicted forces with more appropriate experiments for capturing forces (i.e. rigid cylinder configuration instead of flexible). Overall, similar to the motion, the wake dynamics of the upstream riser can have a significant influence on the exerted forces of the downstream riser.

REFERENCES

[1] Holmes, S., Oakley O. H. and Y. Constantinides, "Simulation of Riser VIV Using Fully Three Dimensional CFD Simulations", OMAE2006-92124, 2006

[2] Constantinides Y, and Oakley O. H, "Numerical Prediction of Bare and Straked Cylinder VIV", OMAE2006-92334, 2006

[3] Allen, D.W. and Hennin, D.L., "Vortex-Indcued Vibration Current Tank Tests of Two Equal-Diameter Cylinders in Tandem", Journal of Fluids and Structures, 17, 767-781, 2003.

[4] Assi, G.R.S, Meneghini, J.R., Aranha, J.A.P., Bearman, P.W., and Casaprima, E., "Experimental Investigation of Flow-Induced Vibration Interference between Two Circular Cylinders", Journal of Fluids and Strucrures, 22, 819-827, 2006.

[5] Papaioannou, G.V., Yue, D.K.P., Triantafyllou, M.S. and Karniadakis, G.E., "On the Effect of Spacing on the Vortex-induced Vibrations of Two Tandem Cylinders", Journal of Fluids and Structures, 24, 833-854, 2008.

[6] Zdravkovich, M.M., "Flow Induced Oscillations of Two Interfering Circular Cylinders", Journal of Sound and Vibration, 101, 511-521, 1985.

[7] AcuSolve, General Purpose CFD Software Package, Release 1.7e, ACUSIM Software, Mountain View, CA, 2008.

[8] Spalart, Deck, Shur, Squires, Streletes & Travin, "A New Version of Detached-Eddy Simulation, Resistant to Ambiguous Grid Densities", Journal of Theoretical & Computational Fluid Dynamics, 20, 181-195, 2006.